Electron Ion Collider

Jaroslav Adam
Czech Technical University in Prague

High Tatras, December 9 – 13, 2024

Triggering Discoveries in High Energy Physics III

Electron Ion Collider (EIC)

- Polarized *ep* and *e*-ions up to 18×275 GeV
- One of RHIC beams is re-used as hadron beam
- Two rings for electrons, accelerator and storage ring
- Detector experiment (ePIC) at location of current STAR, second experiment possible
- First data early 2030s

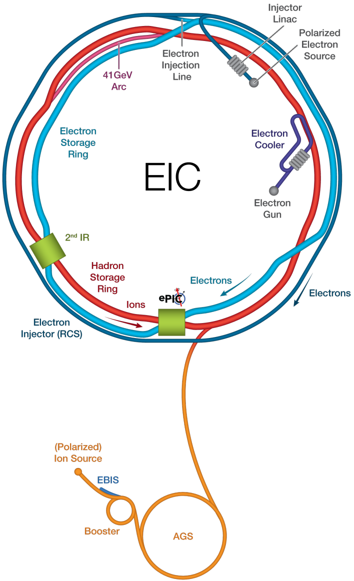

ePIC detector (Electron-Proton/Ion Collider Experiment)

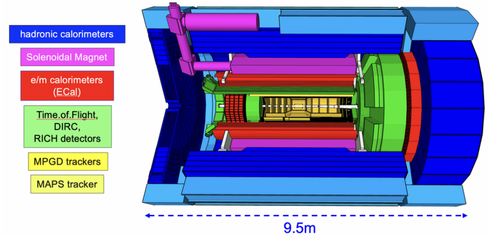

Physics case for the EIC

- Spin and mass composition of nucleons (*proton spin puzzle*)
- QCD dynamics in unexplored kinematic regions
- Jet interactions in cold nuclear matter
- Electroweak physics and beyond the standard model

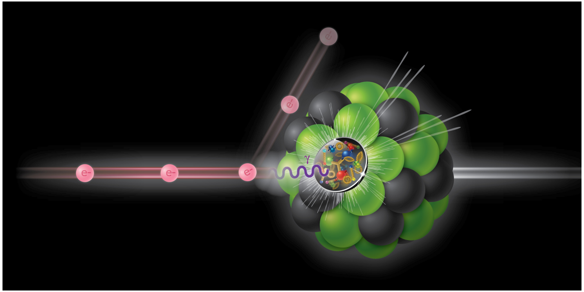

Looking into a nucleus at the EIC

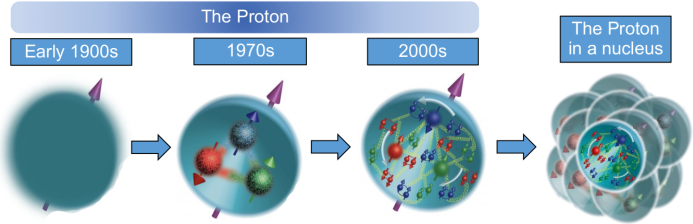
The Proton

Early 1900s

1970s

2000s

The Proton
in a nucleus

Energies and beam species

Species	Energy (GeV)	$\sqrt{s}$ (GeV)
ep	18×275	140.7
	10×275	104.9
	10×100	63.2
	5×100	44.7
	5×41	28.6
eAu	18×110	89.0
	10×110	66.3
	5×110	46.9
	5×41	28.6

- +all hadron species as at current RHIC
- High luminosity $10^{33} - 10^{34}$ $\mathrm{cm^{-1}s^{-1}}$, 100 – 1000× more than HERA
- Integrated 10–100 $\mathrm{fb^{-1}}$ / year

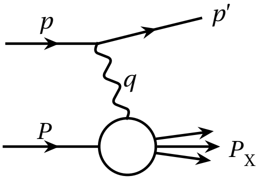

General DIS process

Resolution (virtuality) Q^2:

$$Q^2 = -(p - p')^2$$

Parton momentum fraction x:

$$x = \frac{Q^2}{2Pq}$$

Unprecedented coverage in x and Q^2

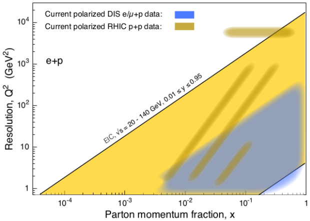

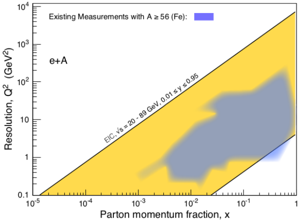

The ePIC experiment (Electron-Proton/Ion Collider Experiment)

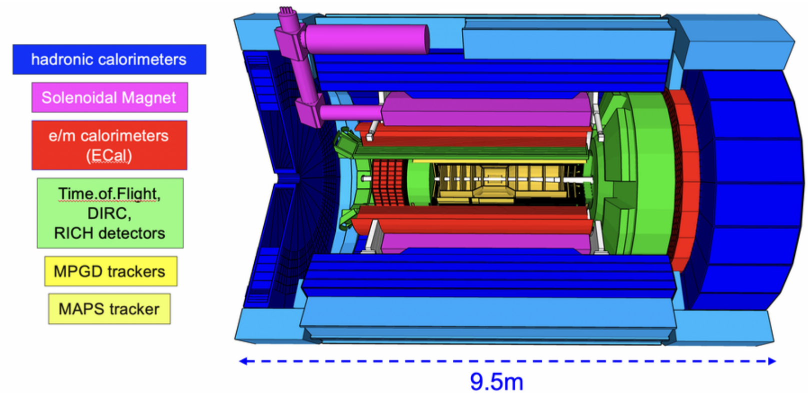

Hermetic coverage for tracking, particle identification and calorimetry in asymmetric collisions

ePIC collaboration

- 850+ participants
- 177 institutions
- 26 countries
- 650+ members active in ePIC

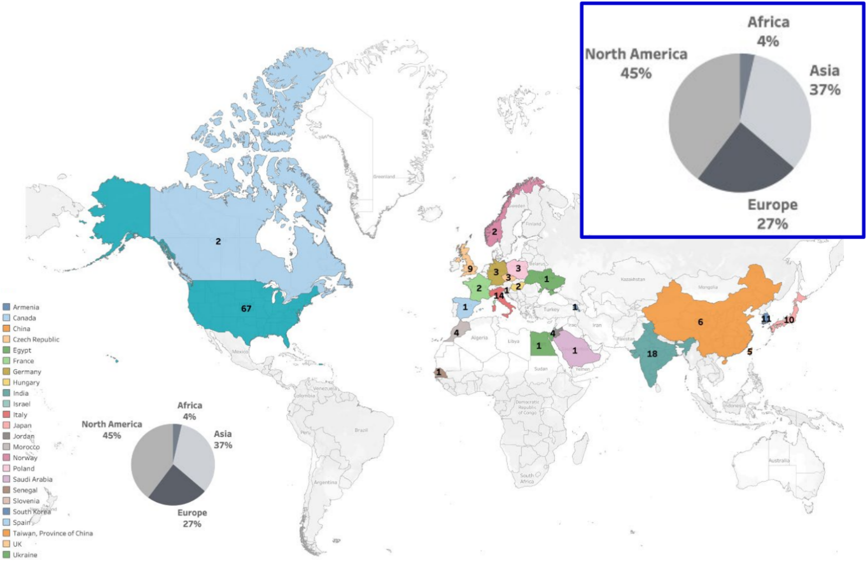

Detector requirements for ePIC experiment

- **Vertex detector:** precise spatial resolution, low material budget
- **Central and endcap trackers:** particle momenta (with help of solenoid magnet)
- **Particle identification:** $\pi/K/p$ separation for each track
- **Calorimeters:** eletromagnetic and hadron
- **DAQ:** streaming readout

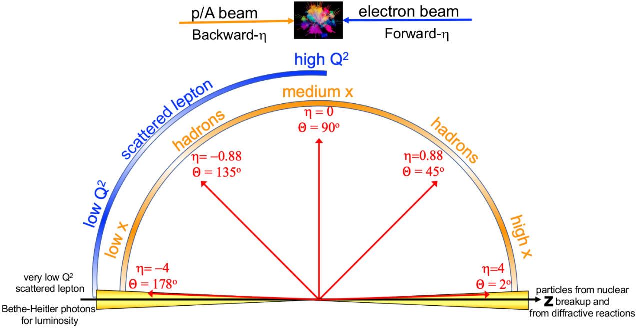

- **Far-forward and backward detectors:** scattered particles at very small angles, luminosity measurement, nuclear breakup

Coordinate convention for ePIC:

- Forward – proton/ion beam direction, $z > 0$
- Backward – electron beam direction, $z < 0$

Central ePIC detectors

Vertex + tracking

- Si and gaseous sensors
- 1.7 T solenoid field

Particle identification

- AC-LGAD for time-of-flight
- Cherenkov hpDIRC and RICH

Calorimeters

- Electromagnetic and hadron parts
- Full enclosure around tracking and identification detectors
- Homogeneous and sampling calorimeters

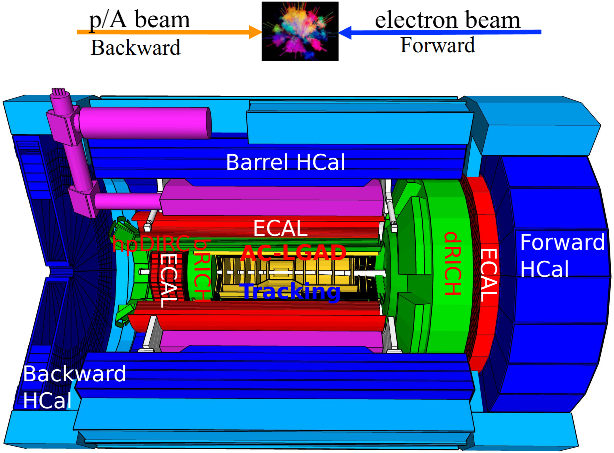

Meeting the requirements within space constraints

Central tracking detectors, $|\eta| < 3.5$

- 6 Si layers (MAPS) + forward/backward disks
- Gaseous µRWell and µMegas
- TOF identification with AC-LGAD

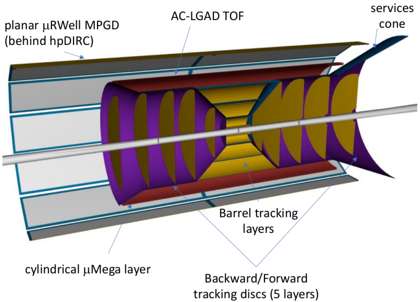

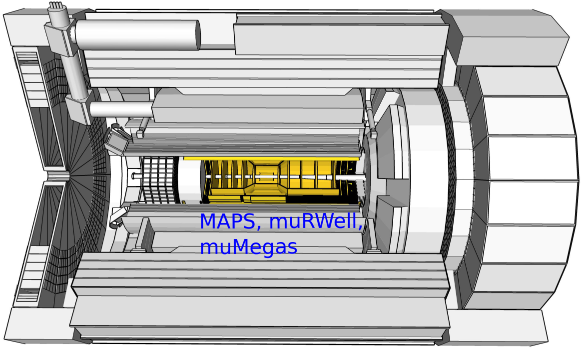

Collision vertex (resolution 3 mm), charged particle momentum (resolution 1%), time-of-flight identification

Layout for central tracking

- MAPS (Monolithic Active Pixel Sensor)
  - Based on 65 nm CMOS, developed with ALICE ITS3
- MPGD (Micro Pattern Gaseous Detector)
  - Connection between tracking and particle identification

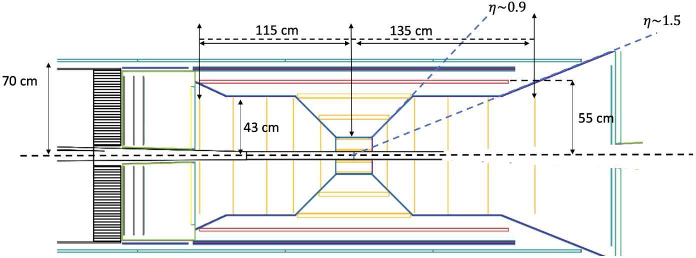

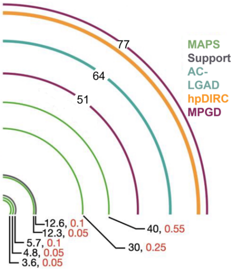

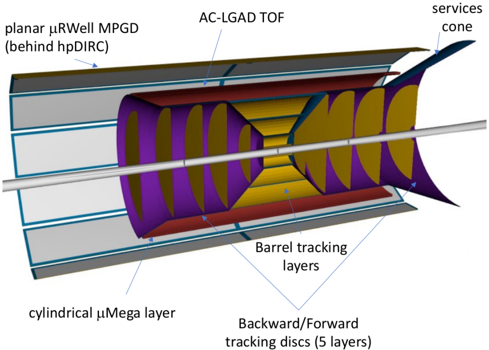

Particle identification

- Time-of-flight (AC-LGAD) and Cherenkov detectors

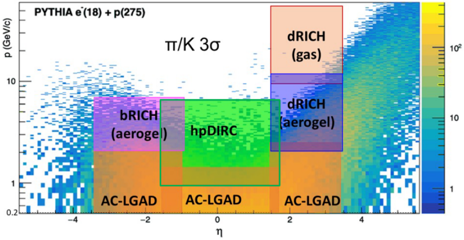

Expected momentum (p) and pseudorapidity (η) distribution

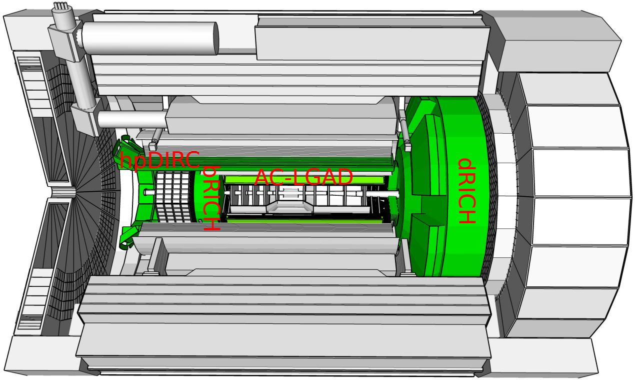

Complete coverage in particle momenta and pseudorapidity

Particle identification by time-of-flight

- AC-LGAD - structure of Low Gain Avalanche Diodes with capacitive (AC) coupling
- 100% fill factor, timing resolution ~30 ps

Barrel layer

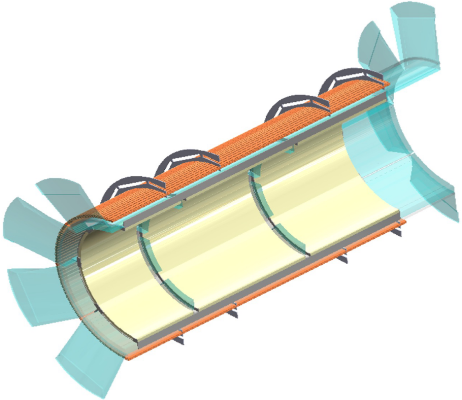

AC-LGAD structure

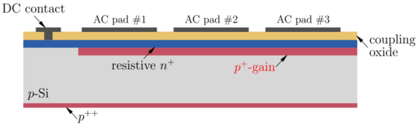

Forward disk

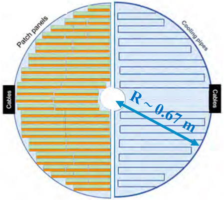

Particle identification by Cherenkov detectors

- Identification by combination of Cherenkov angle and momentum for each track
- Cherenkov radiators, readout by HRPPD (backward), MCP-PMT (barrel) and SiPM (forward)

Backward proximity focusing RICH

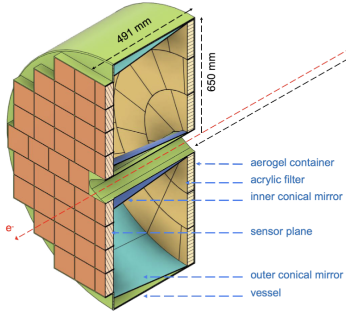

High-Performance DIRC (barrel)

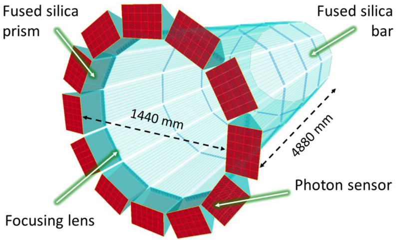

Forward dual-radiator RICH

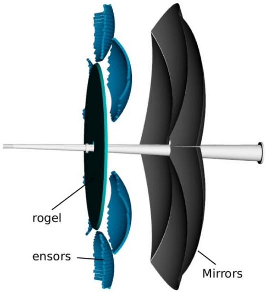

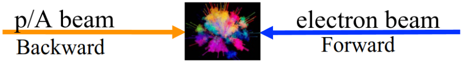

Calorimeters in ePIC detector

- Complete EM and hadron calorimeters in central region and forward (hadron) endcap
- Tail-catcher for hadron calorimeter in backward endcap

Electron / hadron separation, jet reconstruction

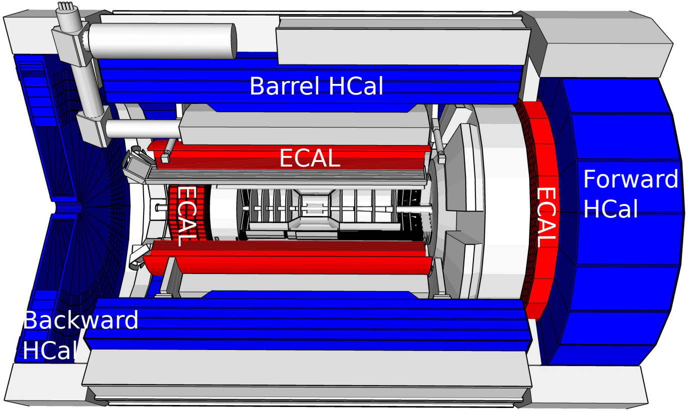

Barrel electromagnetic calorimeter

- Scintillating fibers (SciFi) in Pb absorber
- Imaging layers based on AstroPix sensors

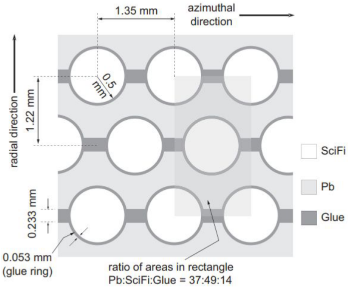

ratio of areas in rectangle Pb:SciFi:Glue = 37:49:14

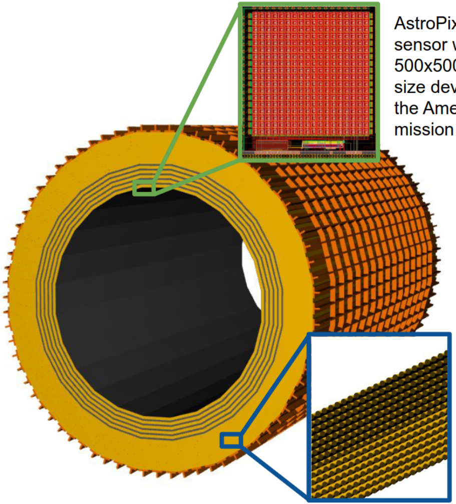

AstroPix: silicon sensor with 500x500μm^2 pixel size developed for the Amego-X NASA mission

ScFi Layers with two-sided SiPM readout

Forward and backward electromagnetic calorimeters

- **Forward ECAL:**
  - WScFi structure
  - Tungsten powder and scintillating fibers
  - SiPM readout
- **Backward ECAL:**
  - PWO crystals
  - SiPM readout

Electron/pion and $2\gamma/\pi^0$ separation

Forward endcap

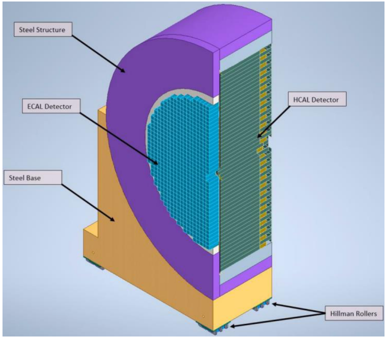

Backward ECAL

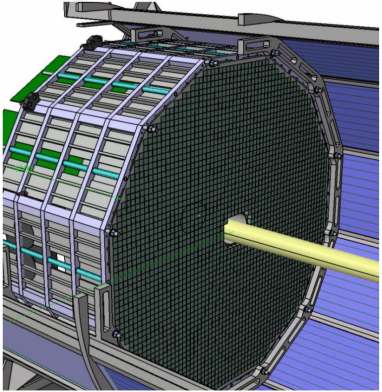

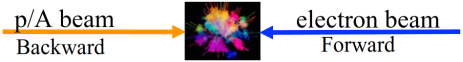

p/A beam

Backward

electron beam

Forward

Hadron calorimeters

- Absorber layers and scintillator tiles + SiPM

Jet kinematics reconstruction

Backward HCal

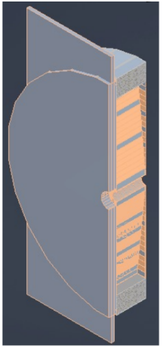

Barrel HCal

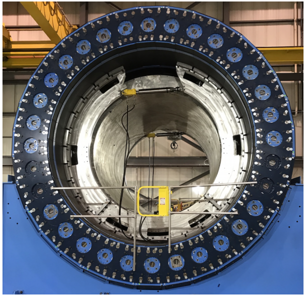

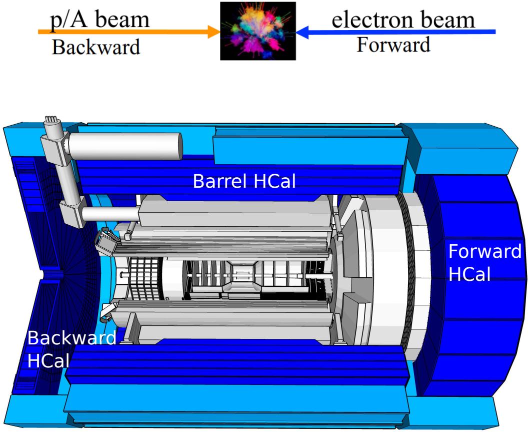

Far-forward / backward detectors

- Particles scattered at small angles, outside central detector
- Detectors are placed along beam magnets

Far-forward ($z \gg 0$)

- Hadron beam direction
- Tracking and calorimeters

Far-backward ($z \ll 0$)

- Electron beam direction
- Luminosity measurement, electrons at low-Q^2

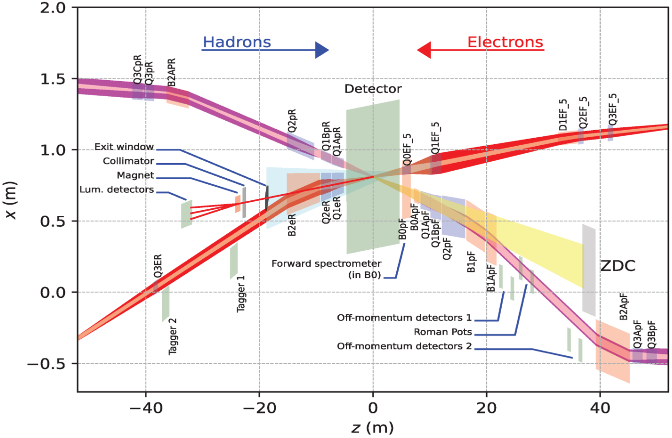

Interaction region layout, note different range in horizontal (x) and longitudinal (z) directions

Far-forward layout

- Roman Pots (RP) for very forward hadrons
- Off-Momentum Detectors (OMD) for nuclear breakup and Λ decays
- ZDC for neutrons and low-energy photons
- B0: tracker and calorimeter inside beam magnet

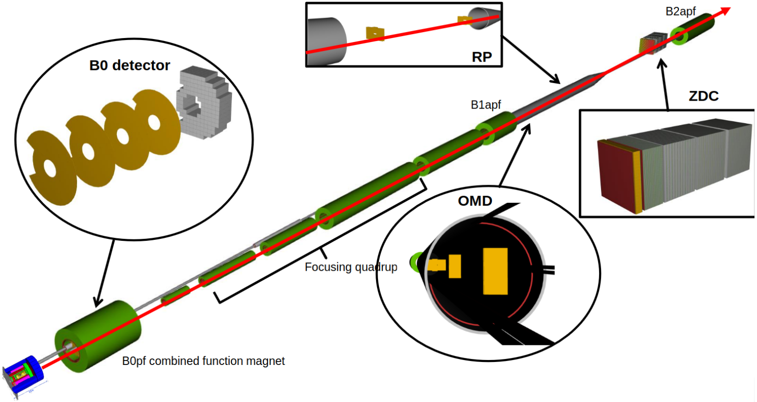

Diffractive processes, spectators in e+A collisions, nuclear excitation and breakup

The drawing is illustrative, not to scale

Far-forward detectors

B0 detector

- 4 Layers of AC-LGAD (charged tracking)
- PWO/LYSO crystals for calorimeter (γ and π^0)

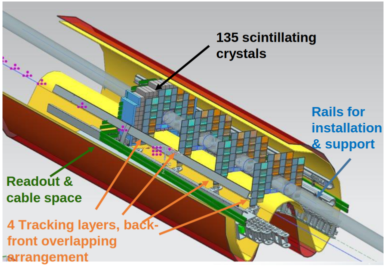

Roman Pots + OMD

- AC-LGAD sensor
- Part of outgoing hadron beampipe

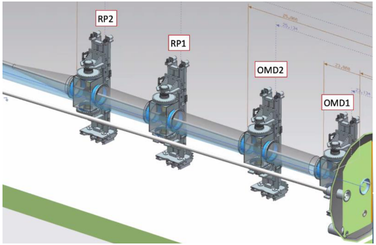

ZDC

- Electromagnetic and hadron parts
- Forward neutrons and π^0/γ separation

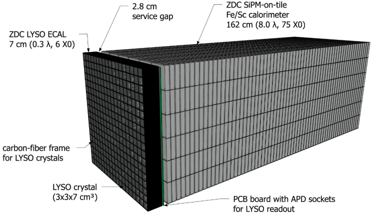

Far-backward region, luminosity measurement

- γ photons from Bethe-Heitler bremsstrahlung, $ep(A) \to e\gamma p(A)$
- Cross section is well known from QED
- Two methods to count the γ photons:

1. Direct γ calorimeter (γ cal)
   - Approximate γ counts
   - Online collider performance
2. Conversion pair spectrometer (PS)
   - Precise counts for physics
   - γ conversions to e^+e^- pairs
   - Dipole magnet, trackers and calorimeters

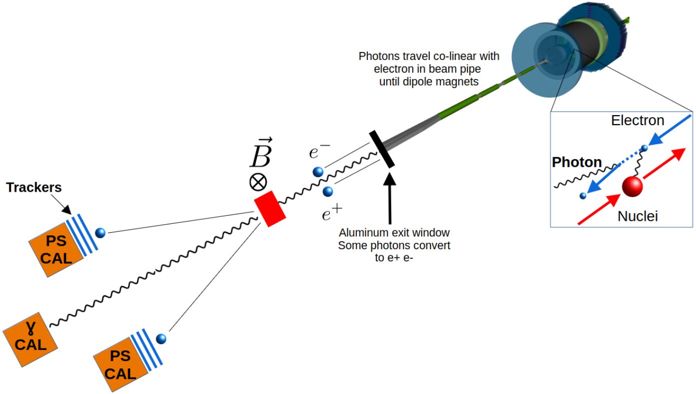

Key part to all cross section measurements (most of EIC physics program), target precision of 1%

Far-backward region, low-Q^2 electron tagging

- Two tagger stations (-20 m) and (-35 m) from interaction point (IP)
- Timepix4 tracker and EM calorimeter

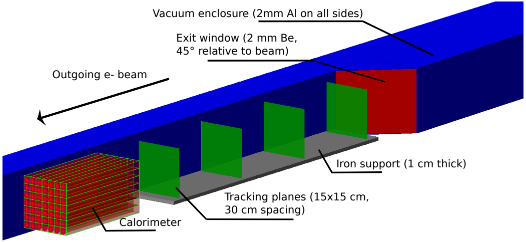

Detail at one of tagger stations

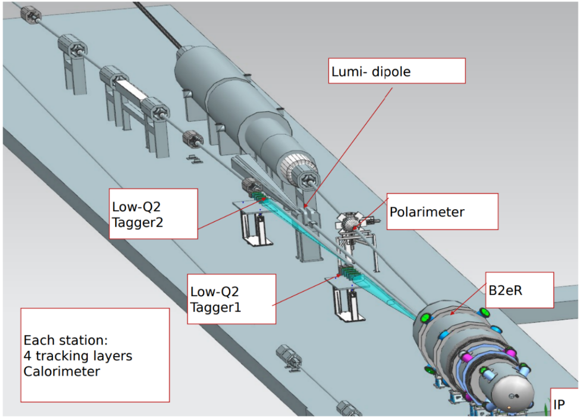

Each station:
4 tracking layers
Calorimeter

Photoproduction physics at low-Q^2 and luminosity precision (coincident e^- and γ detection)

Streaming DAQ

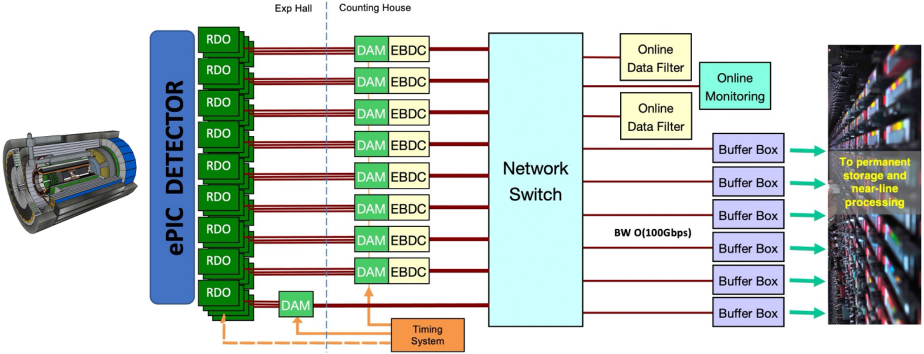

Continuous digitization for all detector data, no external hardware trigger

- All signals passing zero-suppression threshold, timestamp for unique identification
- Detector specific front end boards, commercial high-performance (EBDC) servers

Streaming DAQ workflow

- Specific ASICs in Front End Boards (FEBs)
- Individual detector hits by Readout boards (RDO)
- Optical bidirectional connection to Data Aggregation and Manipulation (DAM) boards
- Clock distribution by Global Timing Unit (GTU)
- The GTU provides accelerator bunch crossing system clock to all front-end systems
- Bunch crossing every 10.15 ns (98.5 MHz)
- Top interaction rate of 500 kHz (exception of luminosity/low-Q^2 having signals every bunch xing)

Data from different detectors are synchronized into packets corresponding to a selected time frame, then sorted into events / bunch crossings

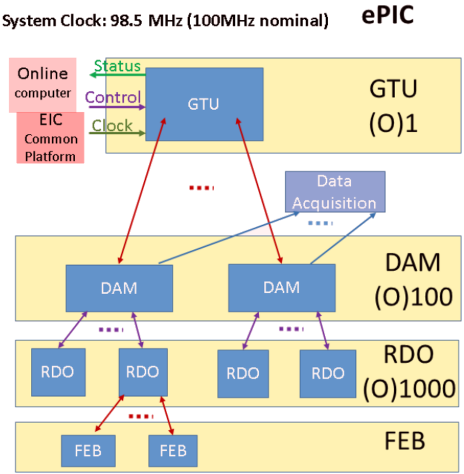

Measurement categories at the EIC

Inclusive DIS

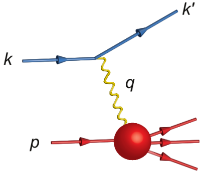

- Scattered electron needs to be detected for event kinematics

Exclusive DIS

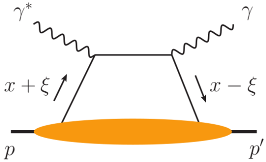

- DVCS or vector meson
- All particles detected with high precision

Semi-inclusive DIS

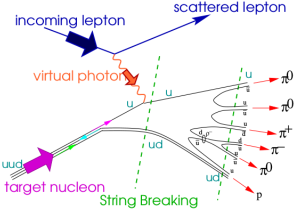

- At least one hadron in coincidence with scattered electron

Electro-weak processes

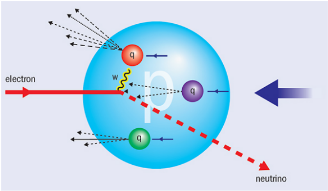

- Electron-quark interaction by $W^{\pm}$ boson
- No scattered electron

Proton spin puzzle

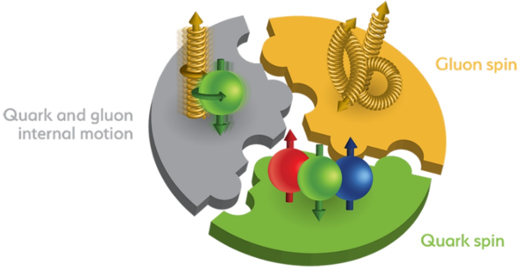

$$\frac{1}{2} = \underbrace{\frac{1}{2}\int_0^1 \mathrm{d}x\Delta\Sigma(x,Q^2)}_{\text{Quark spin}} + \underbrace{\int_0^1 \mathrm{d}x\Delta G(x,Q^2)}_{\text{Gluon spin}} + \underbrace{\int_0^1 \mathrm{d}x\left(\sum_q L_q + L_g\right)}_{\text{Orbital angular momentum}}$$

- Proton (and all hadrons) spin is carried by valence and sea quarks, gluons and their angular momentum

All parts add to 1/2 for a proton at all times, large uncertainties for individual contributions

Proton spin at EIC by longitudinal double-spin asymmetry

- Relative difference in semi-inclusive DIS cross sections between parallel and anti-parallel orientations

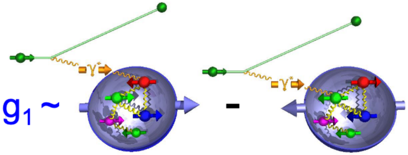

- The asymmetry is related to polarized structure function g_1:

$$\frac{\mathrm{d}\sigma^{++} - \mathrm{d}\sigma^{+-}}{\mathrm{d}\sigma^{++} + \mathrm{d}\sigma^{+-}} \propto g_1(x, Q^2)$$

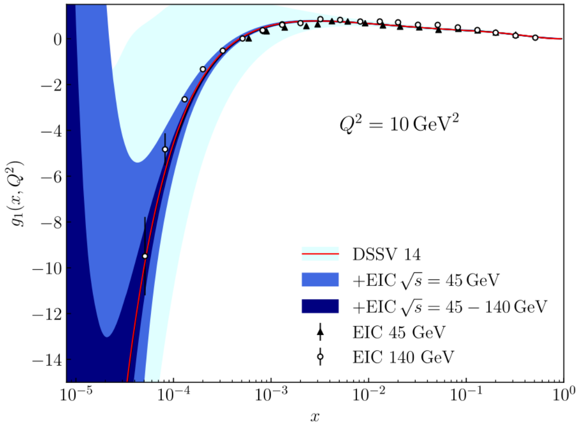

Considerable reduction of uncertainties for gluon and sea quark parts of the spin is expected

Phys.Rev.D 102 (2020) 9, 094018

Nuclear structure

- Quarks and gluons behave different in nuclei
- Quantified by nuclear ratio R^A as ratio of cross section on nucleus to $A\times$ scaled result on proton:

$$R^A_{F_2} = \frac{F_2^A(x, Q^2)}{AF_2^{\text{nucleon}}(x, Q^2)}$$

- $R^A \neq 1$ indicates presence of nuclear effects

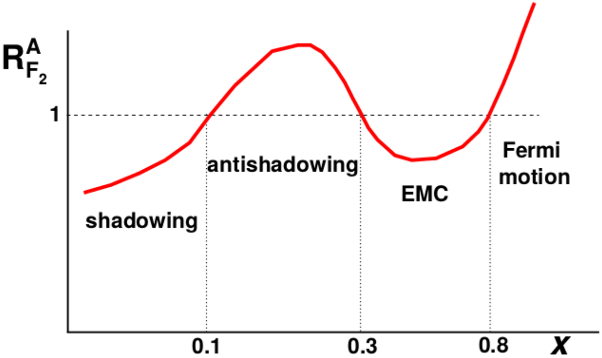

Current estimates at low $x \lesssim 10^{-2}$ (shadowing region) at low scale Q^2 have large uncertainties; new accurate data are needed

Nuclear structure functions at EIC

Inclusive DIS (left) and photon-gluon fusion producing $c\bar{c}$ (right)

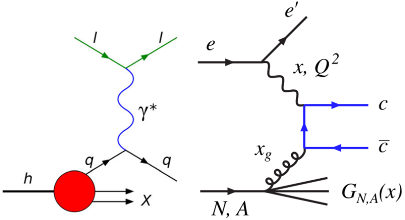

- Cross section measurement allows to extract the structure functions
- Gluon structure is sensitive to non-linear effects

Inclusive DIS

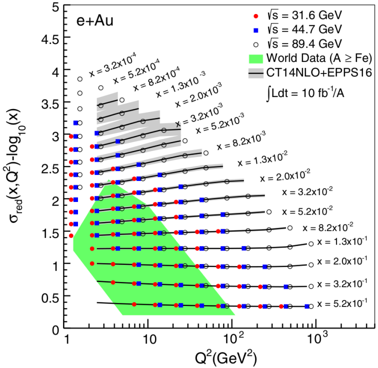

$c\bar{c}$ in photon-gluon

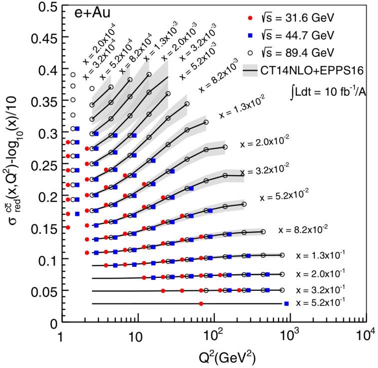

Kinematic coverage and high precision is promising for strong experimental constraints

Phys.Rev.D 96 (2017) 11, 114005

Gluon saturation

- Gluon density steeply increases at larger energies (and lower *x*)

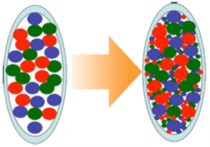

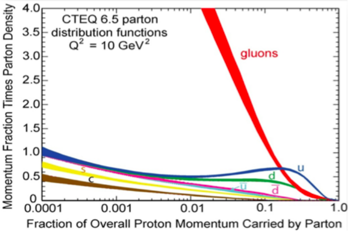

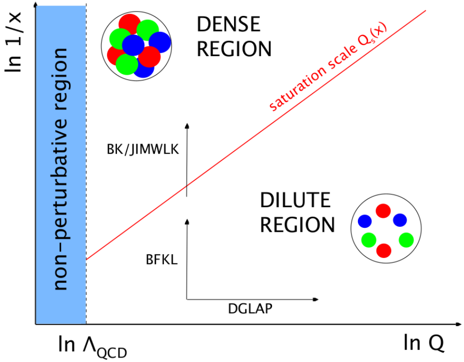

- Still more gluons become present at decreasing momentum fraction *x*

QCD expects an onset of non-linear effects to prevent further growth in density (saturation)

pos.sissa.it/284/001

Probing the gluon saturation at EIC

- Relative differences between linear and nonlinear approach to F_2 and F_L structure functions:

$$\frac{F_{2,L}^{\mathrm{BL}} - F_{2,L}^{\mathrm{Rew}}}{F_{2,L}^{\mathrm{BL}}}$$

- Black dots show initial matching of both approaches at x-Q^2 before expected saturation

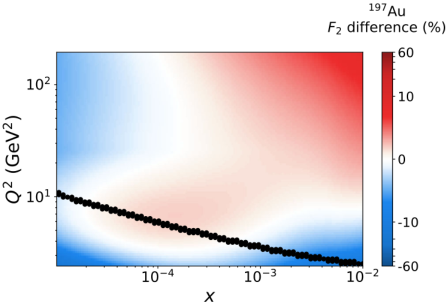

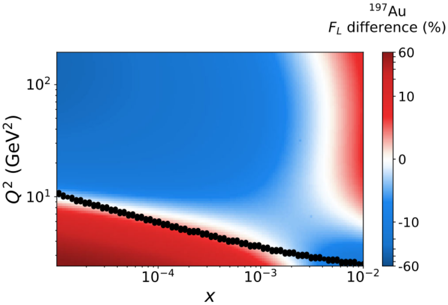

Nuclear longitudinal structure function F_L is well sensitive to saturation at low Q^2

Phys.Rev.D 105 (2022) 11, 114017

Jet interactions in cold nuclear matter

Jet is initiated inside the nucleus; propagates through varying amount of nuclear matter

- Nuclear structure and evolution of parton showers is probed by jet modification
- Final jet is formed by hadronization in nucleus
- EIC will provide data on jets in e-A

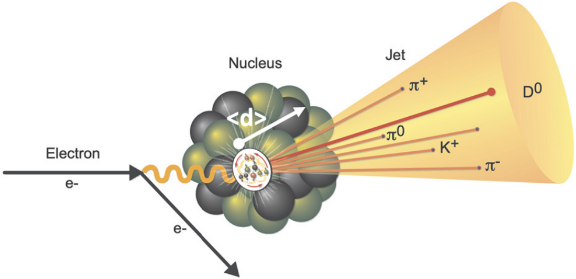

Phys.Lett.B 848 (2024) 138354

Jets in cold nuclear matter

- Nuclear effects to jets are quantified by ratio R_{eA}
- The R_{eA} is a ratio of jet cross sections in η and p_T in e-A to ep

It is possible to distinguish initial parton distribution and final-state interactions contributing to final R_{eA}

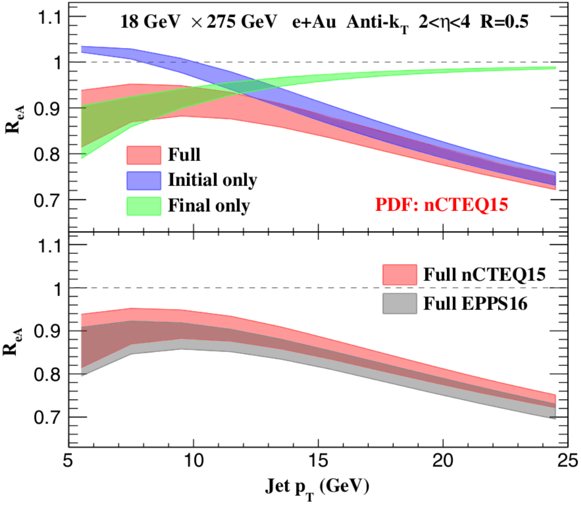

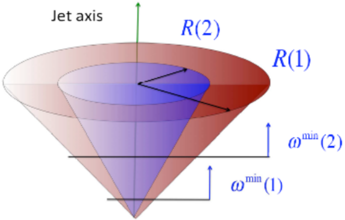

Phys.Rev.Lett. 126 (2021) 25, 252001

Summary

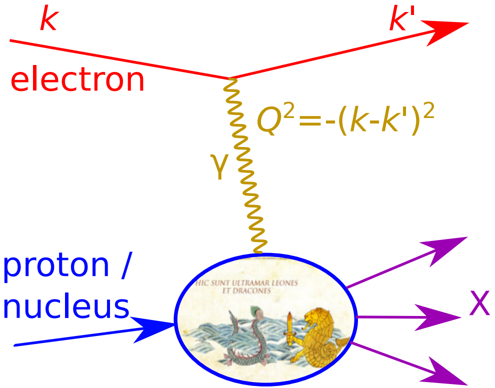

Here be lions and dragons

On schedule to explore the unknown and to go where no one has gone before